TOXICOLOGICAL SCIENCES **78,** 276–286 (2004)
DOI: 10.1093/toxsci/kfh105
Advance Access publication March 10, 2004

Induction of CYP1A1 in Primary Rat Hepatocytes by 3,3′,4,4′,5-Pentachlorobiphenyl: Evidence for a Switch Circuit Element

C. Tenley French, William H. Hanneman,[1] Laura S. Chubb, Ruth E. Billings, and Melvin E. Andersen[2]

Department of Environmental and Radiological Health Sciences, Colorado State University, Fort Collins, Colorado 80523

Received October 7, 2003; accepted November 17, 2003

In vivo **induction of CYP1A1 in hepatocytes by aryl hydrocarbon receptor agonists is heterogeneous. Using immunohistochemistry, cells appear to be either induced or not induced as if the response of an individual cell is better represented as a switch. We have examined induction of CYP1A1** ***in vitro*** **in primary rat hepatocytes to distinguish the responses of populations of cells and responses of individual cells. Cells were treated with various concentrations of the aryl hydrocarbon receptor agonist, 3,3′,4,4′,5-pentachlorobiphenyl. Concentration-response and time-course responses were determined for the population of cells by Western blotting for CYP1A1 protein and by real-time RT-PCR for CYP1A1 mRNA. Individual cell responses were visualized by immunocytochemistry (ICC) for protein and by** ***in situ*** **hybridization (ISH) for mRNA. CYP1A1 mRNA was quantified by frequency distribution analysis of grains observed on the ISH slides. Population responses showed time- and concentration-related increases in induction. Single cell responses appeared as all-or-none in the field, with cells appearing to be induced and others appearing to be not induced. Even at the highest concentrations (2.5×10^{-7} M), some hepatocytes remained unresponsive. Distribution frequencies of single cell induction were more consistent with a switch with variable levels of induction in cells depending on treatment concentration. Combined with the reports from** ***in vivo*** **studies, our results support a switch with rheostat behavior for individual hepatocytes. Mechanistic studies in liver cell lines that are confirmed to exhibit switch-like induction of single cells will be necessary to assess the molecular pathways of this circuit element.**

Key Words: **polychlorinated biphenyl; CYP1A1; hepatocytes.**

Studies elucidating the biological factors that determine the shape of the dose-response curve are crucial for low-dose extrapolations of risk (Farland, 1996). Knowledge of the molecular events that serve as obligate precursor steps for toxic effects may also enable extension of the dose-response curves to lower exposure levels. TCDD (2,3,7,8-tetrachlorodibenzo-*p*-dioxin) is the most potent member of a family of xenobiotics that interact with a specific transcriptional regulatory molecule, the aryl hydrocarbon receptor (AhR) to cause a variety of toxic responses in animals and humans. In the recently completed United States Environmental Protection Agency risk assessment for dioxins there were extensive discussions of approaches for extrapolations of risk for these compounds to low doses. Initial interactions of dioxin-like ligands with the dioxin-binding site on the AhR may be linearly related to concentrations of these ligands. However, there are many events which follow receptor binding (Whitlock, 1999). Thus, more complex dose-response relationships are likely to ensue for downstream events associated with dissociation of the AhR-TCDD unit from the endogenous receptor complex, AhR phosphorylation, heterodimerization with the transcriptional partnering protein, cofactor recruitment, or histone remodeling. In addition, none of these molecular events, by themselves, is necessarily predictive of cellular or organ level responses.

Cytochrome P450 proteins are a superfamily of enzymes involved in the biotransformation of various drugs, carcinogens, and steroid hormones (Estabrook, 1996). A hallmark of exposure of laboratory animals to AhR-agonists is induction of drug metabolizing enzymes, especially the cytochrome P4501A and 1B family enzymes. The dose-response for hepatic induction of CYP 1A1 is a favorite for dose-response analysis, since it has a low level of constitutive expression and a robust increase with maximal induction (Vanden Heuvel *et al.*, 1994). Induction can be represented at the level of a population of cells or at the level of individual cells. Total induction of protein or mRNA in a population of cells could be assessed by Western blots for protein or by RT-PCR for mRNA in homogenates of cells or tissue from treated animals. Alternatively, the induction response could be evaluated on the basis of individual cells in a population *in vitro*, or in a tissue by immunohistochemistry for protein, or by *in situ* hybridization to visualize mRNA in individual cells. These two distinct methods of describing induction (i.e., homogenate versus individual cells) would be similar if the average response of individual cells was similar to the population response. For instance, 50% of maximal induction in the intact liver should

[1] To whom correspondence should be addressed at Department of Environmental and Radiological Health Sciences, Physiology Building (1680) Room 132, 1680 Campus Delivery, Fort Collins, CO 80523-1680. Fax: (970) 491-7569. E-mail: Hanneman@colostate.edu.

[2] Current address: CIIT-Centers for Health Research, Six Davis Drive, PO Box 12137, Research Triangle Park, NC 27709.

represent 50% induction of each of the treated cells. However, *in vivo* responses of populations of cells and individual cells are strikingly disparate.

Immunohistochemical staining of CYP1A1 in the rat liver following *in vivo* treatment with TCDD demonstrates that low doses induce CYP1A1 solely within the centrilobular region (Andersen *et al.*, 1995; Tritscher *et al.*, 1992). As the dose increases, the pattern of induction spreads out toward periportal areas. Within the induced liver, there is a clear boundary between responsive regions (Bars and Elcombe, 1991; Bars *et al.*, 1989). Hence, individual hepatocytes appear as either uninduced or fully induced at any specific dose of TCDD. This regional specificity in induction with increasing dose within the liver is also observed for other enzyme inducers that act through very different molecular pathways, including phenobarbital and clofibrate. With increasing dose *in vivo*, the primary change is the increased area of the acinus over which induction was observed. Physiologically based pharmacokinetic (PBPK) models for regional induction (Andersen *et al.*, 1997a,b) were developed based on presumptions of differences in binding constant for TCDD to AhR within various acinar regions in the liver. These models successfully captured both the responses of the individual hepatocytes within regions and the average response of the intact liver. However, this model lacked biological detail on the mechanistic basis of the differential sensitivity of individual cells.

The observation, *in vivo*, of a distinctly heterogeneous pattern of enzyme induction within the rat liver indicated a binary response (i.e., cells are either induced or remain in a basal state) at the level of signal transduction or gene transcription. To characterize the nature of this pathway for enzyme induction more efficiently, we have examined induction in primary hepatocytes with a prototypical AhR-agonist, 3,3′,4,4′,5-pentachlorobiphenyl (PCB 126). Other work in our laboratory has demonstrated that this compound, as expected, produces regional induction in the liver *in vivo* (Andersen *et al.*, 2002). Thus, the hypothesis underlying our work was that, *in vitro*, CYP1A1 hepatic protein induction would also exhibit a binary switching response. Following treatment with PCB 126, populations of hepatocytes showed a concentration-response for sensitivity to induction. However, induction within individual cells results in either the fully induced phenotype or cells remaining in the basal state. Thus, our expectation is that the mode of induction of both the protein and mRNA in primary hepatocytes *in vitro* resembles the *in vivo* behavior, both qualitatively and quantitatively. The suitability of the *in vitro* model as a surrogate for the *in vivo* system will be determined by analyzing the induction of CYP1A1 by PCB 126 at both the level of mRNA and protein and comparing induction in cell populations and individual cells. Population analysis is through Western blots for protein and real-time RT-PCR for mRNA. Responses of individual cells are evaluated through application of immunocytochemistry and *in situ* hybridization for CYP1A1 protein and mRNA, respectively.

MATERIALS AND METHODS

Establishment of Rat Primary Hepatocyte Cell Culture

Hepatocyte isolation. Adult, male, Sprague-Dawley rats were deeply anesthetized with isofluorane injected, ip with heparin, and the liver perfused with Buffer A at 37°C (35–40 ml/min) for 5–7 min. Buffer A consists of 500 ml of Earle's Balanced Salt Solution (EBSS) with phenol red, without $CaCl_2$ and $MgCl_2$, with 7.5 mM HEPES, 100 nM dexamethasone, 0.5 mM EGTA (ethylene glycol-bis(β-aminoethylether)-N,N,N′N,-tetraacetic acid), 100 units/ml penicillin, and 100 μg/ml streptomycin. When the perfusate was free of blood, a second perfusion with Buffer B, a collagenase buffer, was initiated, using the same perfusion flow rate over 5–12 min at 37°C. Buffer B consists of 500 ml of EBSS (with phenol red, without $CaCl_2$ and $MgCl_2$), 10 mM HEPES, 2.5 mM $CaCl_2$, 100 nM dexamethasone, 100 units/ml penicillin, 100 μg/ml streptomycin, and 0.04% type IV collagenase (Sigma), added just prior to use. The liver was excised and stirred for 1.5 min to release the cells. Cells were then filtered through a 100-micron mesh screen (EC588–100, Sigma). The cell suspension was centrifuged at $50 \times g$ (500 rpm) for 2 min, and the pellet was resuspended in Hepatocyte Wash Buffer (Gibco) containing 100 nM dexamethasone, 100 units/ml penicillin, and 100 μg/ml streptomycin; this wash was repeated twice. For final resuspension, Hepatocyte Attachment Buffer (Modified William's E Media with Nuserum from Gibco, proprietary) was used. Prior to plating, cells were counted, and the viability was assessed using trypan blue. Only isolations yielding a viability of 80% and greater were plated and treated. The concentration of cells was adjusted to 750,000 cells/ml. Cells were plated onto 60-mm dishes or onto each side of two-chamber slides in volumes of 4 ml (3×10^6 cells) and 1.5 ml (1.125×10^6 cells), respectively. Plates and slides were precoated with rat-tail collagen type I (Collaborative Biomedical Products).

In vitro treatment with PCB 126. Cells were incubated at 37°C, 5% CO_2 for 3–3.5 h to allow attachment. At this time, the cells were washed and exposed to Hepatocyte Attachment Buffer without serum, which contained the designated PCB 126 concentrations. PCB 126 was obtained from Accustandard and confirmed to be pure and free of other congeners. PCB 126 was added in DMSO, with the final DMSO concentration being 0.2%. PCB 126 concentrations were initially chosen based on previous experiments with various congeners (Wolfe and Marquardt, 1995). PCB 126 was added to hepatocytes at concentrations ranging from 2.5×10^{-7} to 2.5×10^{-13} M. All subsequent time-course studies were conducted at 2.5×10^{-9} M. The cells were exposed for 24 h for the concentration-response studies and for 1–24 h for the time course study. Limited studies were conducted for longer time periods (48 h and 72 h). The viability of cells following culture was measured at each time point using a lactate dehydrogenase (LDH) assay. Cell viability after culture was at least 75% for all of the studies described.

Responses of Populations of Hepatocytes

Western blots. Five plates of cells per study group were collected for microsomal preparations. Following a wash, 1.5 ml cold potassium phosphate buffer, pH 7.5, was added and the cells were scraped into the buffer with a cell scraper. The cells were homogenized with a handheld polytron and centrifuged at $12{,}000 \times g$ for 10 min. The supernate, containing the microsomes, was then centrifuged at $100{,}000 \times g$ (38,000 rpm) for 1 h. The resulting pellet was sonicated in homogenization buffer. The protein concentration was determined with a protein BCA (Pierce) assay. Microsomes were separated by electrophoresis on a commercially prepared polyacrylamide gel (10% Tris-HCl, Bio-Rad). Following electrophoresis, the gel was rinsed in deionized water, and proteins were electrically transferred to a nitrocellulose membrane (Bio-Rad) in transfer buffer (50 mM Tris base, 38.6 mM glycine, 20% methanol) for 2 h at 80 V. The nitrocellulose membrane was then placed in 5% nonfat dry milk in Tris buffered saline–Tween 20 (TBS-T), to block nonspecific proteins, and incubated at 4°C overnight. TBS-T was made of Tris buffered saline (100 mM Tris base, 18 mM NaCl, pH 7.6) and 0.1% Tween 20. Subsequently, blots were incubated with a rabbit polyclonal anti-rat CYP1A1 antibody (Chemi-

con), diluted 1:500 in 0.5% nonfat dry milk, on a rocker for 1 h. Following the primary antibody incubation, blots were washed with TBS-T three times for 3 min each and incubated with 1:5000 anti-Rabbit IgG, horseradish peroxidase conjugate (Sigma) for 1 h at room temperature. A chemiluminescent detection system employing luminol as a substrate for horseradish peroxidase was used. Chemiluminescence was captured on film, and immunoreactive bands were visualized on an AlphaImager™ Documentation and Analysis system.

Total RNA isolation and reverse transcription (RT). Total RNA was isolated from hepatocyte cultures, using guanidinium thiocyanate by the method of Chomczynski and Sacchi (1987). Briefly, cells plated on a 60-mm plate were washed in PBS and extracted with 400 μl "solution D" (4 M guanidinium thiocyanate, 25 mM sodium citrate pH 7.0, 0.5% lauryl sarcocinate, 0.1 M 2-mercaptoethanol) on ice. Subsequently, 40 μl of 2 M sodium acetate, pH 4.0, 400 μl phenol/chloroform and 4 μl isoamyl alcohol were added to the samples and they were vortexed. Samples were centrifuged at 10,000 $\times$ *g* for 20 min at 4°C. The RNA was then purified by washing in ice-cold ethanol three times and reconstituted in DEPC water. The concentration and purity of RNA was evaluated spectrophotometrically and on a 1.5% agarose gel. One μg of total RNA was reverse transcribed using the Promega Reverse Transcription system containing oligo(deoxythymidine)$_{15}$ primers (0.5μg), AMV (avian myeloblastosis virus) reverse transcriptase (15 units), dNTP mix (1 mM each), first strand buffer (10 mM Tris-HCL, 50 mM KCl, 0.1% Triton X-100), $MgCl_2$ (5 mM), and recombinant RNasin ribonuclease inhibitor (10 units) in a final reaction volume of 20 μl. The reaction was incubated at 42°C for 15 min and then 99°C for 5 min. The cDNA samples were stored at −20°C until used. Negative controls for the RT reaction utilized reactions with no AMV reverse transcriptase enzyme.

Real-time quantitative polymerase chain reaction (PCR). Quantitative PCR of the cDNA samples was performed with the Bio RAD iCycler iQ™ Real-Time Detection System. PCR was conducted with primers for the CYP1A1 gene and for the β-actin housekeeping gene. Dr. Nigel Walker (NIEHS) kindly provided primer and Taqman probe sequences. These sequences are shown in Table 1. The cDNA (50 ng) was amplified in a mixture of 1 mM dNTPs (2-deoxynucleoside 5-triphosphates), 0.5 μM each of forward and reverse primers, 0.2 μM Taqman probe primers, PCR buffer "F" (Invitrogen), and 1 unit Platinum Taq polymerase (Invitrogen) in a 50 μl total reaction. The fluorescent moieties of the Taqman probe primers were 5′ 6-FAM™ and 3′ Black Hole Quencher™-1 synthesized by Integrated DNA Technologies Inc. Conditions of the PCR were an initial melting step at 95°C for 3 min followed by 50 cycles of 95°C for 15 sec and 55°C for one min. Negative controls for all experiments used water instead of cDNA for the PCR reaction. The lack of DNA contamination was indicated by using negative controls for the RT reactions. Calculation of fold induction was conducted as described by others (Martinez *et al.*, 2002; Rose'Meyer *et al.*, 2003). The data was normalized by subtracting the difference of the C_T values between the CYP1A1 gene of interest and the β-actin housekeeping gene. This calculation of (cyp1a1 C_T)–(β-actin C_T) is ΔC_T. Fold induction (relative expression) was calculated as $2^{-(S\Delta C_T - C\Delta C_T)}$ where $S\Delta C_T$–$C\Delta C_T$ is the difference between the sample ΔC_T (PCB 126 treated) and the control ΔC_T (DMSO, vehicle control). Based upon cDNA concentration curves, both the CYP1A1 and β-actin reactions amplified at the same efficiency, which approached 100%.

Responses of Individual Primary Hepatocytes

Two-chambered slides of cells were immediately fixed in 1% paraformaldehyde diluted in phosphate buffered saline (PBS) for 10 min and washed in PBS for 10 min. Slides were allowed to air dry and kept at 4°C until later use.

Immunocytochemistry (ICC). Immunocytochemistry was used to determine CYP1A1 protein levels in individual cells and was performed on duplicate slides for each treatment group. On the day of staining, slides were rehydrated and incubated in 0.3% hydrogen peroxide, immersed in Citra Antigen Retrieval Solution (Biogenex), and microwaved until just boiling. They were then microwaved at 30% power for 10 min and allowed to cool. After a 5-min wash in running deionized water, the slides were incubated in PBS for 5 min, then with Avidin blocking solution (Vector Labs) at 37°C for 15 min, followed by a quick spray off with PBS and Biotin blocking solution (Vector Labs) for 15 min at 37°C. After another quick wash, slides were incubated for 10 min with normal goat serum from Vectastain Avidin-Biotin Complex (ABC) kit (Vector Labs). Polyclononal rabbit anti-rat Cyp1A1 antibody (Chemicon) was added at 1:1000 for 15 min at 37°C. After a 5-min wash in PBS, biotinylated anti-rabbit IgG antibody was added (Vectastain kit) for 25 min. Then slides were washed for 5 min in PBS, and ABC reagent (Vectastain kit) was added for 30 min. Following another 5-min wash in PBS, 3-amino-9-ethylcarbazole (AEC, Biomeda) was prepared and added for approximately 5 min at 37°C, then washed off with deionized water. The slides were then counterstained for 1 min with Gill's hematoxylin and washed in running tap water for 5 min. Slides were cover-slipped and visualized on a Bioquant® Imaging System (R&M Biometrics, Nashville, TN).

Generation of CYP1A1-specific RNA probes. The mouse CYP1A1 cDNA clone used to generate the RNA probe was obtained from Dr. Dan Nebert (University of Cincinnati). It did not cross-hybridize with CYP1A2 (Dey *et al.*, 1999). We subcloned this 3′-specific cDNA fragment into a pGEM-3 vector and then transformed it into *E. coli*. The plasmid was isolated, and restriction enzyme digests identified the cDNA vector. The cDNA clone was sequenced and confirmed to be CYP1A1 via a BLAST search of the GenBank database. Primers were designed to include SP6 and T7 sites on the flanking ends. PCR was used to amplify the 544-bp segment, and the amplicon product was isolated from a TAE 1.5% agarose gel and purified with a phenol/chloroform extraction and ethanol precipitation. Transcription of the single-stranded, ^{35}S-labeled cRNA probe was achieved using 0.1 μg of the cDNA template, 320 μCi uridine 5′-(α^{35}S-thio)triphosphate, SP6 and T7 polymerases (30 units), RNAse inhibitor (20 units), dithiothreitol (DTT, 10 mM), NTPs (1.5 mM each), cold UTP (1:20), and SP6/T7 transcription buffer in a 10-μl reaction. The SP6 polymerase transcribed the antisense probe, while the T7 polymerase transcribed the sense probe to serve as a negative control. The radiolabeled cRNA probe was ethanol precipitated and confirmed by polyacrylamide gel electrophoresis (5% acrylamide, 7.5% urea), and the incorporated radioactivity was determined. Percent incorporation of ^{35}S-UTP ranged from 33% to 70%.

In situ hybridization (ISH). Hepatocytes fixed with paraformaldehyde were kept at 4°C for a maximum of 5 days until the hybridization procedure was conducted. Slides were allowed to come to room temperature, washed in PBS, and acetylated with acetic anhydride (0.25% in tetraethylammonium). Slides were rinsed in 2× standard sodium citrate solution (SSC, 20× stock is 3 M sodium chloride, 0.3 M trisodium citrate) for 10 min and dehydrated with a series of ethanol washes: 70, 80, 95, and 100%. After air-drying the slides, they were hybridized for 20 h at 65°C in buffer (50% formamide, 0.1% sodium

TABLE 1
Primer sequences used in Real Time RT-PCR

Gene	Forward primer	Reverse primer	Taqman probe
CYPIA1	5′-tcaaagagcactacaggacatttg	5′-gggttggttaccaggtacatgag	5′-aagggccacatccgggacatca
β-actin	5′-gacaggatgcagaaggagattactg	5′-gctgatccacatctgctggaa	5′-atcaagatcattgctcctcctgag

thiosulfate, 100 mM dithiothreitol, 0.5% sodium dodecyl sulphate (SDS), 600 mM NaCl, 20 mM Tris pH 7.5, 0.04% Denhart's, 2 mM ethylenediaminetetraacetic acid (EDTA) pH 8.0, 0.02% salmon sperm DNA, 0.10% total yeast RNA, 0.01% yeast tRNA, 20% dextran sulfate) containing 2×10^7 CPM/ml probe. Following hybridization, the slides were rinsed vigorously in 8 consecutive washes of 2× SSC and treated with 20 μg/ml RNase A for 30 min at 37°C. The slides were then washed in consecutive washes of SSC (final stringency of 57°C, 0.1× SSC), dehydrated, and air-dried. In each of the dehydration steps 1mM dithiothreitol (DTT) and 0.04× SSC was added to the ethanol wash to stabilize the ^{35}S attachment. To visualize the hybridized probe, slides were coated in photographic emulsion (NTB-3, Eastman Kodak) diluted 1:1 in distilled water and exposed for 5 days at 4°C. Slides were developed in Kodak D19 developer, fixed, rinsed in water, and air-dried. They were then counterstained with Gill's hematoxylin for 5 min, washed, and cover-slipped.

Single cell analysis. *In situ* slides were examined under magnification, using a Bioquant® Imaging System to ascertain the degree of labeling. Differences in intensity of CYP1A1 expression were compared by visual comparison and quantitative analysis. For specific time points and concentrations, the intensity of labeling within individual cells was quantified by measuring the density of silver grains using the Bioquant system. The instrument calculated the number of grains per fixed area approximating each cell nucleus and area of cytoplasm. A specific array used to analyze the slides permitted outlining of each cell individually and measurement of the cellular and nuclear area. The threshold was determined separately for each cell, which then allowed for individual measurements of the total grain area and grain area over the nucleus. For each treatment group, ISH was performed on three separate, two-chamber slides. The number of individual cells quantified for each treatment group ranged from 150 to 180.

RESULTS

Populations of Hepatocytes

Time course study: protein. To determine the amount of CYP1A1 protein induced within a culture of treated primary hepatocytes, Western blots were used (Fig. 1). Hepatocytes were treated with 2.5×10^{-9} M PCB 126 for the following lengths of time: 1, 2, 4, 8, 16, and 24 h. A steady increase in the darkness of the bands occurred, reflecting an increase in total protein concentration beginning at 4 h and continuing through 24 h, with no discernible induction at the 1- and 2-h time points.

Concentration-response study: protein. CYP1A1 protein levels were assessed with respect to varying concentrations of PCB 126 treatment, which ranged from 2.5×10^{-13} M to 2.5×10^{-6} M. Western blots were performed on the microsomal extracts from hepatocyte cultures. Blots were visualized on film, and the images were captured with an AlphaImager™ (Fig. 2). Qualitative comparisons between the CYP1A1 protein bands illustrated a clear concentration-dependent response of increased protein induction with increasing concentration. The protein level was almost maximal at the 2.5×10^{-9} M concentration of PCB 126 treatment. In general, the darkness of the CYP1A1 band over multiple experiments increased until 2.5×10^{-9} M and leveled out at the higher concentrations.

Time course study: mRNA. Total RNA from primary hepatocyte populations was analyzed by real-time RT-PCR for the expression of CYP1A1 mRNA. Hepatocytes were treated with 2.5×10^{-9} M PCB 126 for various time points to assess the time point of maximal mRNA induction. The plot of fold induction within a population of hepatocytes at increasing time points reveals the induction increased throughout the 24-h period (Fig. 3). By 16 h, the mRNA induction level had barely surpassed the 50-fold mark. Within the next 8 h, the rate of increase grew, resulting in over 150-fold induction by 24 h. In a separate experiment, cells were treated for 24, 48, and 72 h, and CYP1A1 mRNA was quantified. There was no further increase in mRNA beyond the 24-h time point. All subsequent single-cell assays were conducted using a 24-h PCB 126 treatment.

Concentration-response study: mRNA. Induction of mRNA in response to varying levels of PCB 126 treatment was analyzed quantitatively using real-time RT-PCR. The plot of PCB 126 treatments with CYP1A1 fold induction revealed a sigmoid concentration-response curve of mRNA induction in the hepatocyte population. A maximum fold induction is approached at approximately 2.5×10^{-10} M and maintained throughout the higher concentrations up to 2.5×10^{-7} M (Fig. 4). This observation confirmed that the PCB-induced, CYP1A1 response occurs at the transcriptional level and provided more quantitative data than possible with Western blots. For time-course single-cell assays, a concentration of 2.5×10^{-9} M PCB was chosen, due to the consistent level of induction over multiple experiments.

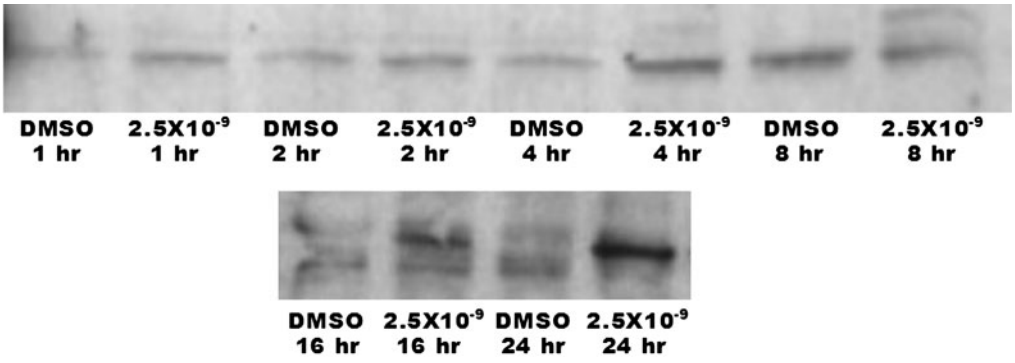

FIG. 1. CYP1A1 protein time-course. Western blot images were captured with an AlphaImager™ 2002 Documentation and Analysis system. Hepatocyte primary cultures were treated with 2.5×10^{-9} M PCB 126 for various time points. Protein was isolated, standardized, and separated on a polyacrylamide gel. Following transfer to a nitrocellulose membrane, CYP1A1 antibody was used to detect CYP1A1 protein. A chemiluminescent detection system was used to capture the bands on film.

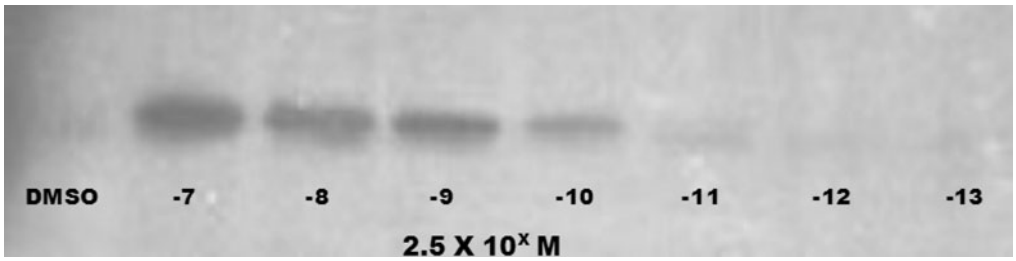

FIG. 2. CYP1A1 protein concentration-response Western Blot images captured with an AlphaImager™ Analysis system. Hepatocyte primary cultures were treated with 2.5×10^{X} M PCB 126 for 24 h. Protein was isolated, standardized, and separated on a polyacrylamide gel. Following transfer to a nitrocellulose membrane, CYP1A1 antibody was used to detect CYP1A1 protein. A chemiluminescent detection system was used to capture the bands on film.

Responses of Hepatocytes at the Level of Single Cells

Qualitative time course and concentration-response studies: protein. CYP1A1 protein induction was assayed on a single-cell basis. Staining of the CYP1A1 protein was compared qualitatively across the various time points at the single PCB 126 concentration of 2.5×10^{-9} M (Fig. 5) and across the different concentrations at the 24-h time point (Fig. 6). Staining of individual cells was evident with both studies and generally indicated that some cells responded and others remained unresponsive. In comparison with the Western blot results, the time-course study (Fig. 5) shows a similar fraction of cells responding at all times, with an increasing level of staining with increased incubation time. Slides from the 1-, 2-, and 4-h time points are similar to DMSO controls, with virtually no induced cells (data not shown).

Concentration-response results (Fig. 6) include representative images from DMSO control and 2.5×10^{-11} M, 2.5×10^{-10} M and 2.5×10^{-9} M and revealed an increase in the number of induced cells with increasing concentration. The slides from 2.5×10^{-13} M and 2.5×10^{-12} M PCB concentrations (not shown) were comparable to control, with no detectable CYP1A1 protein. At a concentration of 2.5×10^{-9} M, there remain cells that are not induced (Fig. 6d). In a separate experiment, cells were treated with higher concentrations of 2.5×10^{-8} M and 2.5×10^{-7} M, and refractory, unstained, cells were still observed (data not shown). Considering the inherent qualitative nature of ICC, further studies to quantify the induction of CYP1A1 in single cells were done with *in situ* hybridization.

Qualitative time course and concentration-response studies: mRNA. CYP1A1 mRNA was analyzed on a cell-by-cell basis through development of an ^{35}S-UTP labeled CYP1A1 cRNA

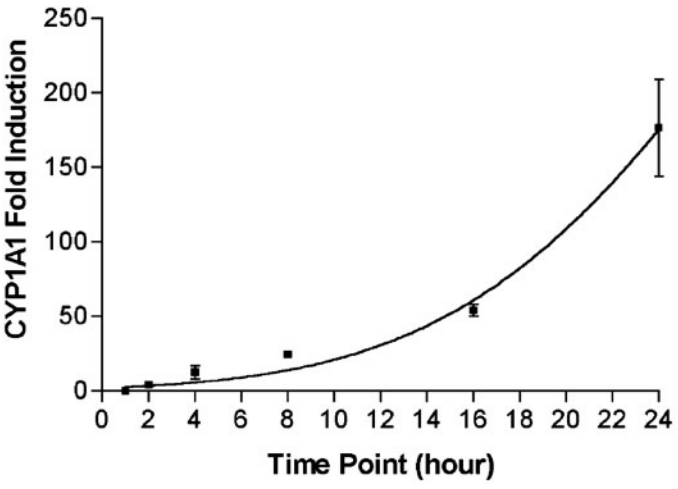

FIG. 3. CYP1A1 mRNA fold induction levels following treatment with 2.5×10^{-9} M PCB 126 for 1, 2, 4, 8, 16, and 24 h. Primary hepatocyte cultures were treated, and the RNA was harvested at the various time points. Real-time RT-PCR using primers specific for the gene of interest, CYP1A1, and a housekeeping gene, β-actin, accomplished relative quantification of the mRNA induction levels. Points represent the mean ± SEM of independent experiments. DMSO control treatments at each time point confirmed an absence of induction.

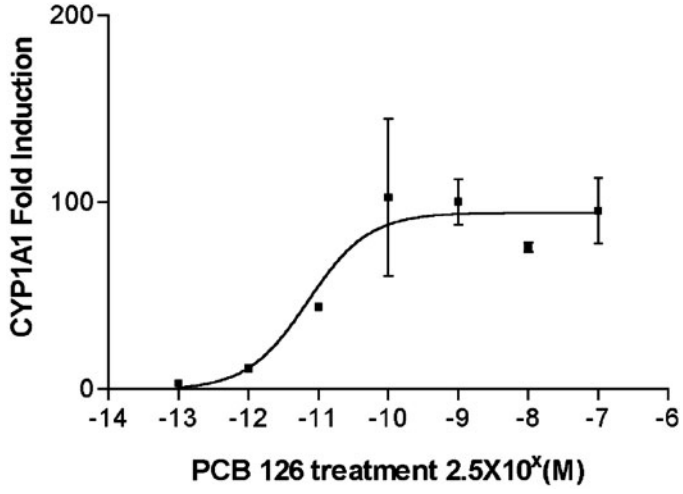

FIG. 4. CYP1A1 mRNA fold induction levels following treatment with PCB 126 for 24 h. Treatment concentrations ranged from 2.5×10^{-7} M to 2.5×10^{-13} M. Primary hepatocytes were isolated, and once plated, the cultures were treated. Total RNA was harvested 24 h later. Relative quantification of the mRNA induction levels was accomplished by real-time RT-PCR using primers specific for the gene of interest, CYP1A1, and a housekeeping gene, β-actin. Points represent the mean ± SEM of independent experiments. DMSO control treatment revealed an absence of induction.

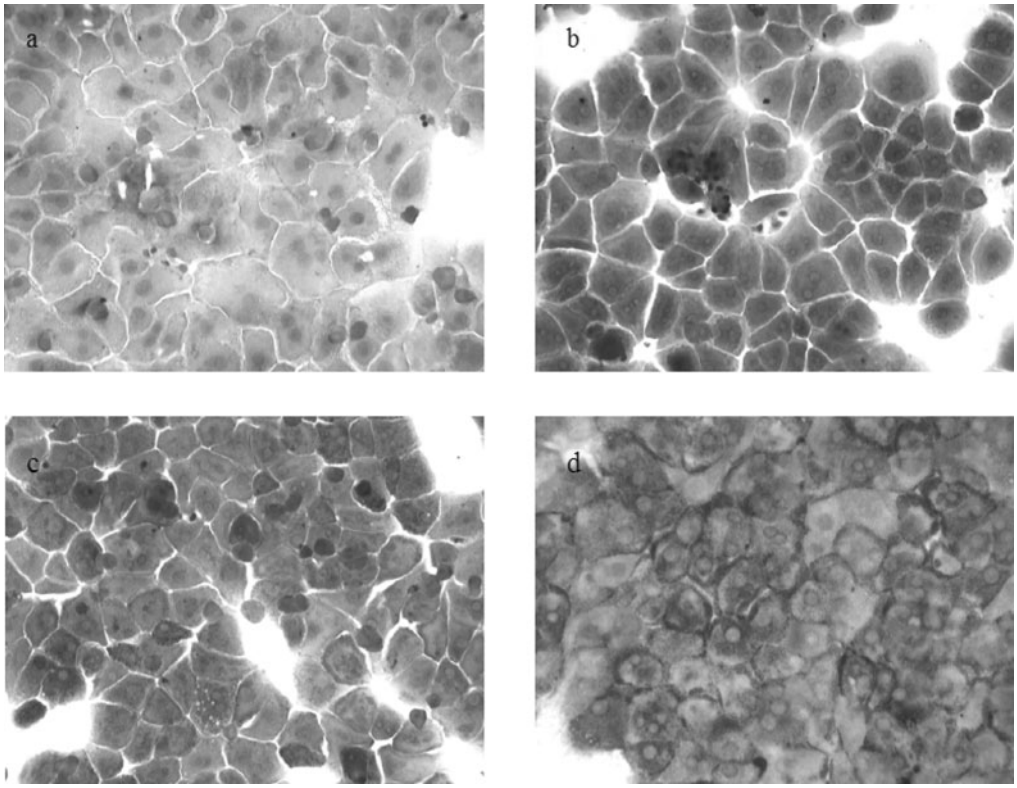

FIG. 5. Immunocytochemistry stained slides reflecting the distribution of induced CYP1A1 protein within rat primary hepatocytes treated with 2.5×10^{-9} M PCB 126 for a time-course analysis. The Gill's hematoxylin counterstained photomicrographs are under 10× magnification. (a) DMSO control; (b) PCB treated, 8 h; (c) PCB treated, 16 h; (d) PCB treated, 24 h.

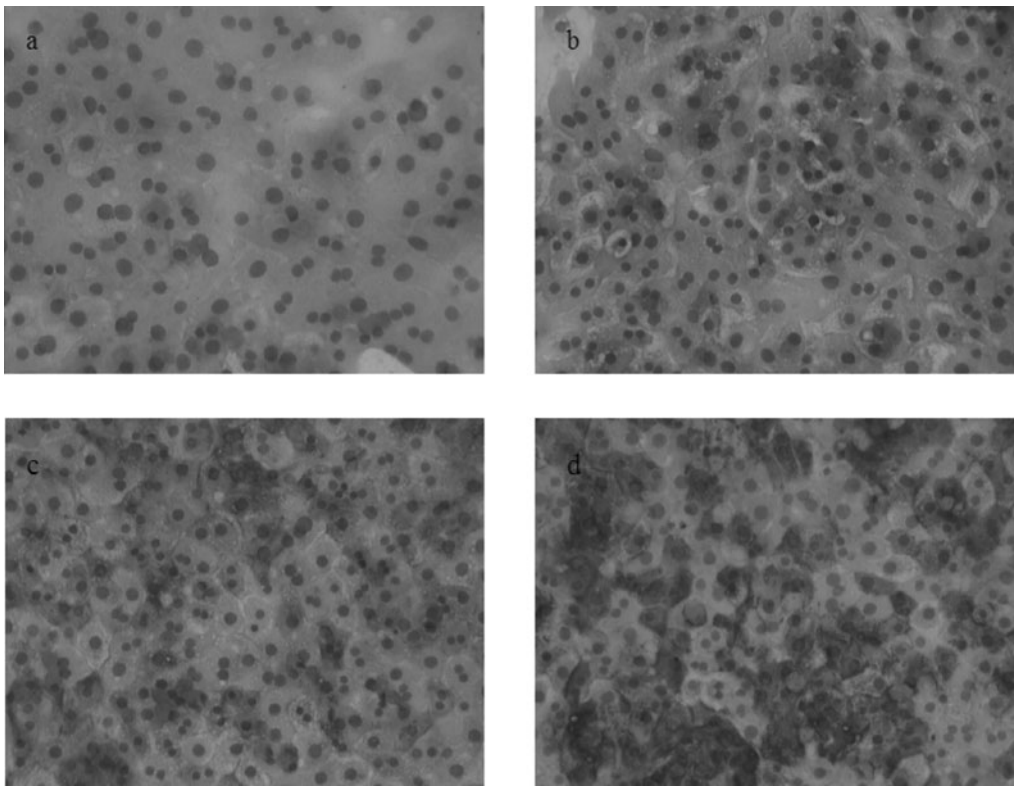

FIG. 6. Immunocytochemistry stained slides reflecting the distribution of induced CYP1A1 protein within rat primary hepatocytes treated with various concentrations of PCB 126 for 24 h. The Gill's hematoxylin counterstained photomicrographs are under 10× magnification. (a) DMSO control; (b) 2.5×10^{-11} M PCB; (c) 2.5×10^{-10} M PCB; (d) 2.5×10^{-9} M PCB.

probe and *in situ* hybridization of PCB 126 treated cells. A sense strand probe served as a negative control and demonstrated no hybridization (not shown). Representative images taken at 40× magnification from each treatment group are shown in Figures 7 and 8. The induction of CYP1A1 mRNA within individual cells can clearly be visualized by hybridization with the ^{35}S-labeled probe, which appears as black grains within the images. Even after accounting for the background staining, induction of CYP1A1 mRNA can be seen on a single-cell basis. In both the time-course study and the concentration-response study, there appeared to be both an increased number of cells covered by grains and a higher density of grains per cell. The induction, however, does not follow a population distribution consistent with two populations — one basal population and one fully induced population. Instead, the responses indicate that the induced state is variable and related to the concentration of the PCB 126. These qualitative conclusions were also tested by developing distributions of staining intensity with Bioquant analysis of the images.

Quantitative time course and concentration-response studies: mRNA analysis. The following quantitative procedure was used. *In situ* slides were analyzed under 40× magnification using a Bioquant® Imaging System, which measured the density of grains within individual cells to ascertain the degree of labeling. The instrument calculated the number of grains per fixed area approximating each cell nucleus and cytoplasm area. The number of individual cells quantified for each treatment group and time point ranged from 150 to 180. The raw data, reflecting the percentages of the cellular and nuclear area occupied by grains, were plotted as frequency distributions using GraphPad® Prism 3.0 (Figs. 9 and 10).

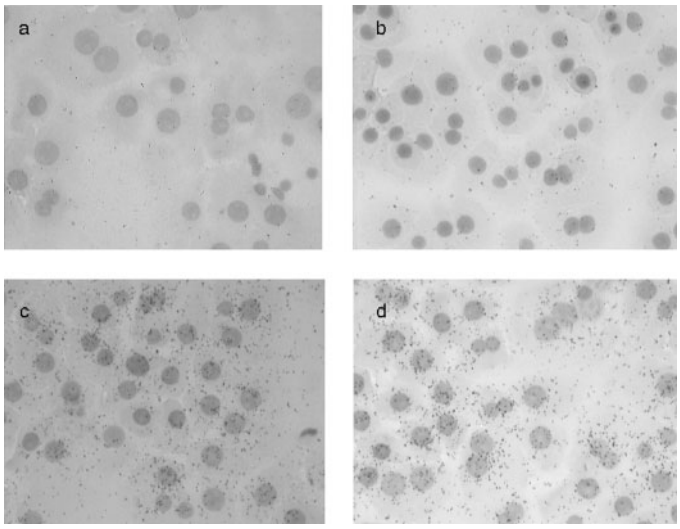

FIG. 7. Distribution of inducible CYP1A1 within rat primary hepatocytes treated with 2.5×10^{-9} M PCB 126 for a time-course analysis. The Gill's hematoxylin counterstained, bright-field photomicrographs are under 40× magnification. (a) DMSO control; (b) PCB treated, 8 h; (c) PCB treated, 16 h; (d) PCB treated, 24 h.

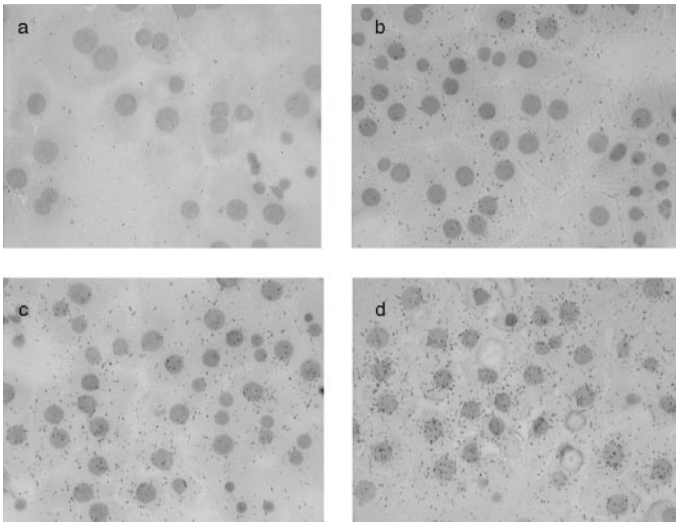

FIG. 8. Distribution of inducible CYP1A1 within rat primary hepatocytes treated for 24 h with varying concentrations of PCB 126 for a concentration-response analysis. The Gill's hematoxylin counterstained, bright-field photomicrographs are under 40×magnification. (a) DMSO control; (b) 2.5×10^{-11} M PCB; (c) 2.5×10^{-10} M PCB; (d) 2.5×10^{-9} M PCB.

Time course frequency distributions (Fig. 9) confirm the trend visualized across the 8-, 16-, and 24-h time points. The graph of the 4-h treatment (not shown) is identical to that of DMSO, except with a few cells containing 2% of their cellular area occupied by CYP1A1 mRNA grains. As seen by the total induction plot (Fig. 3), there is a marked increase in the number of cells that leave the bin associated with basal induction as time increases. The distribution of the induced cells (those that have left the basal induction level) also shifts to the right with increasing numbers of cells in the bins associated with higher levels of mRNA in the cells.

Concentration-response frequency distributions (Fig. 10) revealed a decrease in uninduced cells corresponding to an increase in the number of induced cells across the 2.5×10^{-11} M, 2.5×10^{-10} M, and 2.5×10^{-9} M concentrations. The 2.5×10^{-12} M concentration graph (not shown) is similar to that of DMSO, but with fewer cells in the 0% pool and several cells appearing in the 4% pool. Again, while an increasing number of cells transition from being not induced to induced, the distribution of induction levels varies. In comparison with the hepatocyte population induction results (Fig. 4), there is good correspondence, except that there is a greater difference in the 2.5×10^{-10} M and 2.5×10^{-9} M frequency distributions than the PCR graph suggests. Additionally, the presence of uninduced cells at the 2.5×10^{-9} M concentration indicates that a higher concentration may be required to trigger the threshold for those cells to elicit CYP1A1 mRNA induction or that some of the primary hepatocytes are refractory to induction *in vitro*.

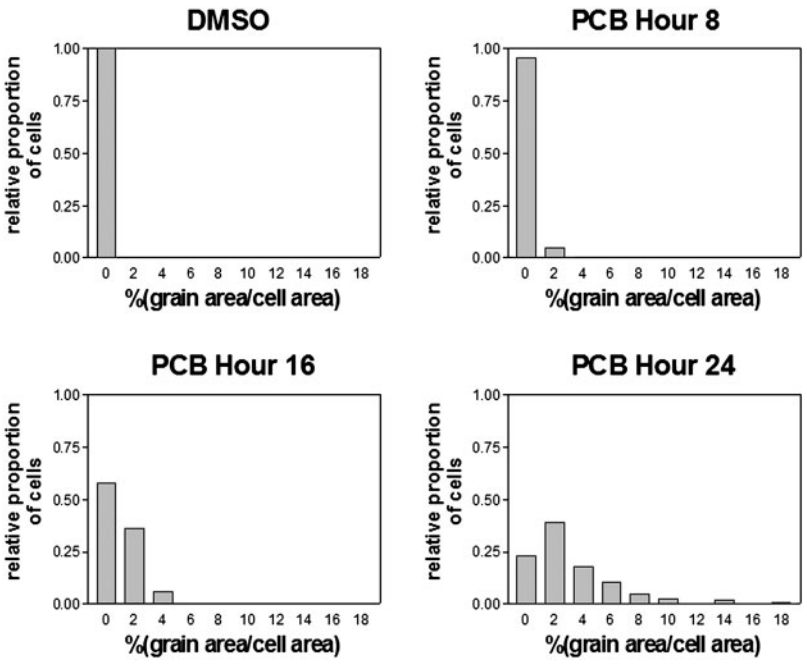

FIG. 9. Frequency distributions of induced CYP1A1 message generated from a quantitative analysis of grain density over individual cells. Rat primary hepatocytes were treated with 2.5×10^{-9} M PCB 126 for various time points and fixed on slides for *in situ* hybridization with ^{35}S-labeled CYP1A1 cRNA probe. Single-cell analysis of expression levels was done on a Bioquant® instrument. (Frequency distribution bin width = 2.0.)

DISCUSSION

Our *in vitro* model evaluating both population and individual cell responses permits better comparison of *in vitro* with *in vivo* observations of induction. In the populations of cells in culture, we observed concentration-related increases in both protein and mRNA, although the degree of induction is much less than reported *in vivo*. Our maximal induction was several hundred-fold. The reported fold-induction *in vivo* is several thousand-fold (Vanden Heuvel *et al.*, 1994). Western blots and real-time RT-PCR confirmed the *in vitro* CYP1A1 induction response at the level of the population of cells.

Analysis of enzyme induction at the level of the individual cell revealed that the induction response appears to operate, for the most part, in a binary fashion. Cells were either uninduced or induced within the fields of observation. This was determined by quantifying CYP1A1 mRNA using *in situ* hybridization. Visually, cells with no induction and highly induced cells were seen in the same field of observation. The ICC, while qualitative, showed that protein induction increased with time at a single concentration and the percentage of cells responding increased with PCB 126 concentration. However, there were still uninduced cells at the highest concentration.

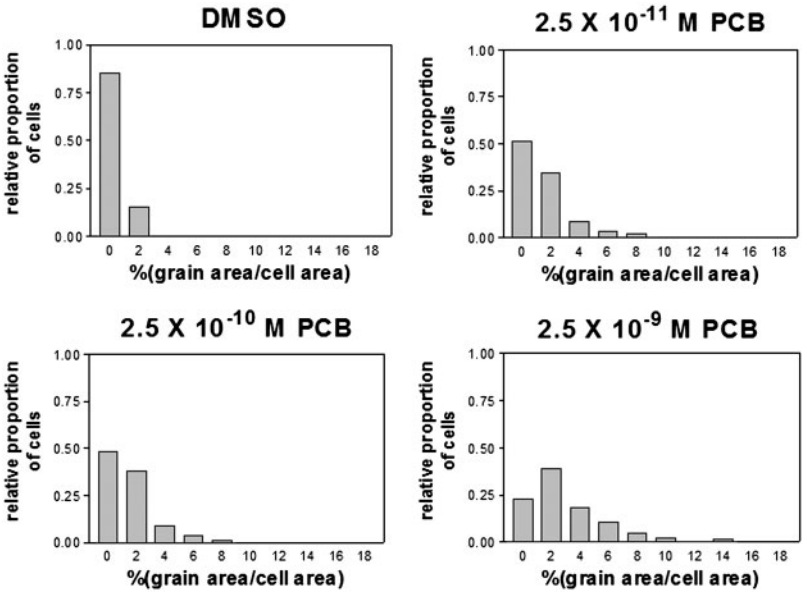

FIG. 10. Frequency distributions of induced CYP1A1 message generated from a quantitative analysis of grain density over individual cells. Rat primary hepatocytes were treated with various concentrations of PCB 126 for 24 h and fixed on slides for *in situ* hybridization with ^{35}S-labeled CYP1A1 cRNA probe. Single-cell analysis of expression levels was done on a Bioquant® instrument. (Frequency distribution bin width = 2.0.)

Our distribution analysis of the responses of single cells was developed based on the studies in which progesterone, acting through surface receptors, induces maturation of *Xenopus* oocytes (Ferrell and Machleder, 1998). Within a population, the oocytes displayed a graded response to progesterone. However, when examined individually for activation of MAP kinase in the oocytes, the response was all-or-none, with an apparent Hill coefficient for steepness of the response of over 30. The estimate of the Hill coefficient was obtained from frequency distributions for the content of activated MAP kinase in individual cells as a function of dosage of progesterone. The all-or-none behavior of the MAP kinase cascade in these oocytes appears to be based on a positive feedback process that creates a switch (Ferrell and Machleder, 1998; Huang and Ferrell, 1996). Other conditions capable of conferring a binary response within signal transduction pathways include inhibition of activators, multistep reaction cascades, and the activity of kinases and phosphatases in phosphorylation and dephosphorylation cycles (Louis and Becskei, 2002).

While signaling cascades provide evidence for some threshold responses, additional investigations suggest gene network involvement in the generation of binary responses (Rossi *et al.*, 2000). Multiple studies now indicate that, at the level of an individual cell, transcription of genes either occurs at a maximal state or not at all (Biggar and Crabtree, 2001; Fiering *et al.*, 2000; Hume, 2000; Ko *et al.*, 1990). For instance, an ample body of evidence labels transcription as a digital process, by which regulation of DNA transcription switches the cell between an on and off mode (Femino *et al.*, 1998; Fiering *et al.*, 1990; Ko *et al.*, 1990; Newlands *et al.*, 1998; Ross *et al.*, 1994; Takasuka *et al.*, 1998; White *et al.*, 1995).

Consistent with expectations for the switching response (Ferrell and Machleder, 1998; Louis and Becskei, 2002), our frequency distributions of single cells showed a gradual decrease in the pool of uninduced cells with increasing concentration and duration of exposure (Figs. 9 and 10). This switching response was accompanied by an increase in the proportion of cells within the induced pool; however, a single, maximal induction peak does not result. Instead, groups of induced cells exhibited varying degrees of induction intensity. Overall, the resulting distributions appear to support a hybrid switching module where a switch works in concert with a rheostat, much like a dimmer on a light switch in a home. The two modules for a switch and a rheostat may represent different aspects of AhR function, with the switch being an obligatory step for expression at any level of ligand-signal (i.e., concentration) and the concentration of the ligand-receptor complex at any concentration determining the extent of induction in a cell that has been switched to an on position.

An important consideration in confirming the existence of a switch and rheostat from this limited *in vitro* model is how well it represents what is actually occurring *in vivo*. In other work in our laboratory (Chubb *et al.*, 2002), *in vivo* experimentation also reveals regions of highly induced cells distinctly separate from uninduced regions. In a qualitative sense, the *in vitro* system consistently models what is seen *in vivo*. The levels of response are comparable, based on the existence of cells in either an on or off state, but with varying degrees of induction. The varying level of induction was noted qualitatively in immunohistochemistry of livers treated with three different doses of PCB 126 (0.1, 1.0, and 10 μg/kg/day) and in preliminary *in situ* hybridization of tissues from these rats (Chubb *et al.*, 2002). While the support for a switch and rheostat in CYP1A1 induction by the AhR is not totally unequivocal, the consistency of the results indicates that it would be important to recast the PBPK model for regional induction to include a switch and rheostat to evaluate the *in vivo* dose-response results for both the total liver and regional distribution of induction. This analysis could be compared with the earlier model that assumed an all-or-none response of hepatocytes (Andersen *et al.*, 1997a). Several molecular circuit arrangements could give rise to these biological switches. Receptor autoinduction embedded in a positive feedback loop has been modeled as a mechanism of generating steep dose-response curves for reporter gene induction (Andersen and Barton, 1998). This strategy appears to be more likely to play a role in control of bacterial operons rather than in mammalian enzyme induction in liver. Ultrasensitivity (steep dose-response behaviors with small changes in input) has been examined in MAP kinase cascades as a source of biological switching (Huang and Ferrell, 1996).

Probing the cascade of reactions leading up to CYP1A1 transcription is crucial to understanding what contributes to the all-or-none character of the switch and rheostat response. With respect to the hepatocyte *in vitro* model, if key enzymes within the signal transduction pathway behave differently between neighboring cells, these differences could potentially lead to generation of both types of responses among the population of cells. A recent study by Bhalla *et al.* (2002) pinpointed a mechanism serving as a locus for determining both a graded and binary response in NIH-3T3 fibroblast cells. The investigators looked at the stimulation of the MAP kinase cascade and demonstrated a system with both bistable and monostable behavior. Mechanistic studies are critical for identifying the processes and or enzymes responsible for generating a particular cellular response. The ultimate goal of mechanistic studies in the context of the *in vitro* system would be to discover potential candidate circuits for a switch locus and possibly decipher whether they are flexible in nature. The AhR-Arnt dimer is an excellent candidate for modulation by nongenomic enzymatic processes. Indeed, the involvement of MAP kinase pathways (ERK and JNK), acting independent of the AhR, are apparently obligatory for subsequent gene expression (Tan *et al.*, 2002). The overall phosphorylation status of both members of the AhR-Arnt heterodimer is crucial in the regulation of resulting signal transduction pathways and transcriptional events (Levine and Perdew, 2001; Long *et al.*, 1999; Park *et al.*, 2000).

The *in vitro* system described here is a valuable tool with which to better assess the nature of the induction response and to probe further into the molecular understanding of ligand-receptor actions. This model provides an important step toward the ultimate goal of quantitatively assessing the mechanisms controlling receptor-mediated induction of xenobiotic metabolizing enzymes within the liver. With the *in vitro* system methodology securely in place, mechanistic investigations should provide further insight into the nature of the cellular response and the variable sensitivity of different liver cell types. In addition, use of liver cell lines might be more seriously considered if they can be shown to undergo a switch-like activation rather than a smooth induction of both population and individual cells. Further emphasis on evaluating the mechanisms of switching will prove valuable in assessing the risks of inducing toxicants and in uncovering potential drug targets within signaling cascades that integrate nongenomic and genomic actions preceding the transcriptional response. These results reinforce the need to examine nonlinear low-dose extrapolation of risk of AhR agonists to account for complex transcriptional regulation by the AhR.

REFERENCES

Andersen, M. E., and Barton, H. A. (1998). The use of biochemical and molecular parameters to estimate dose-response relationships at low levels of exposure. *Environ. Health Perspect.* **106,** 349–355.

Andersen, M. E., Birnbaum, L. S., Barton, H. A., and Eklund, C. R. (1997a). Regional hepatic CYP1A1 and CYP1A2 induction with 2,3,7,8-tetrachlorodibenzo-*p*-dioxin evaluated with a multicompartment geometric model of hepatic zonation. *Toxicol. Appl. Pharmacol.* **144,** 145–155.

Andersen, M. E., Eklund, C. R., Mills, J. J., Barton, H. A., and Birnbaum, L. S. (1997b). A multicompartment geometric model of the liver in relation to regional induction of cytochrome P450s. *Toxicol. Appl. Pharmacol.* **144,** 135–144.

Andersen, M. E., Mills, J. J., Jirtle, R. L., and Greenlee, W. F. (1995). Negative selection in hepatic tumor promotion in relation to cancer risk assessment. *Toxicology* **102,** 223–237.

Andersen, M. E., Yamg, R. H. S., French, C. T. Chubb, L. S., and Dennison, J. E. (2002). Molecular circuits, biological switches and non-linear dose response relationships. *Environ. Health Perspect.* **110** (Suppl.), 971–978.

Bars, R. G., and Elcombe, C. R. (1991). Dose-dependent acinar induction of cytochromes P450 in rat liver. Evidence for a differential mechanism of induction of P450IA1 by beta-naphthoflavone and dioxin. *Biochem. J.* **277,** 577–580.

Bars, R. G., Mitchell, A. M., Wolf, C. R., and Elcombe, C. R. (1989). Induction of cytochrome P-450 in cultured rat hepatocytes. The heterogeneous localization of specific isoenzymes using immunocytochemistry. *Biochem. J.* **262,** 151–158.

Bhalla, U. S., Ram, P. T., and Iyengar, R. (2002). MAP kinase phosphatase as a locus of flexibility in a mitogen-activated protein kinase signaling network. *Science* **297,** 1018–1023.

Biggar, S. R., and Crabtree, G. R. (2001). Cell signaling can direct either binary or graded transcriptional responses. *EMBO J.* **20,** 3167–3176.

Chomczynski, P., and Sacchi, N. (1987). Single-step method of RNA isolation by acid guanidinium thiocyanate-phenol-chloroform extraction. *Anal. Biochem.* **162,** 156–159.

Chubb, L. S., Benjamin, S. A., Painter, J. T., Dean, C. E., Andersen, M. E. (2002). Regional induction of CYP1A1 protein during treatment of rates with mixtures of PCB126 and PCB 153. *Toxicologist* **66,** 93.

Dey, A., Jones, J. E., and Nebert, D. W. (1999). Tissue- and cell type-specific expression of cytochrome P450 1A1 and cytochrome P450 1A2 mRNA in the mouse localized *in situ* hybridization. *Biochem. Pharmacol.* **58,** 525–537.

Estabrook, R. W. (1996). The remarkable P450s: A historical overview of these versatile hemeprotein catalysts. *FASEB J.* **10,** 202–204.

Farland, W. H. (1996). Cancer risk assessment: Evolution of the process. *Prev. Med.* **25,** 24–25.

Femino, A. M., Fay, F. S., Fogarty, K., and Singer, R. H. (1998). Visualization of single RNA transcripts in situ. *Science* **280,** 585–590.

Ferrell, J. E., Jr., and Machleder, E. M. (1998). The biochemical basis of an all-or-none cell fate switch in *Xenopus* oocytes. *Science* **280,** 895–898.

Fiering, S., Northrop, J. P., Nolan, G. P., Mattila, P. S., Crabtree, G. R., and Herzenberg, L. A. (1990). Single cell assay of a transcription factor reveals a threshold in transcription activated by signals emanating from the T-cell antigen receptor. *Genes Dev.* **4,** 1823–1834.

Fiering, S., Whitelaw, E., and Martin, D. I. (2000). To be or not to be active: The stochastic nature of enhancer action. *Bioessays* **22,** 381–387.

Huang, C. Y., and Ferrell, J. E., Jr. (1996). Ultrasensitivity in the mitogen-activated protein kinase cascade. *Proc. Natl. Acad. Sci. U.S.A.* **93,** 10078–10083.

Hume, D. A. (2000). Probability in transcriptional regulation and its implications for leukocyte differentiation and inducible gene expression. *Blood* **96,** 2323–2328.

Ko, M. S., Nakauchi, H., and Takahashi, N. (1990). The dose dependence of glucocorticoid-inducible gene expression results from changes in the number of transcriptionally active templates. *EMBO J.* **9,** 2835–2842.

Levine, S. L., and Perdew, G. H. (2001). Aryl hydrocarbon receptor (AhR)/AhR nuclear translocator (ARNT) activity is unaltered by phosphorylation of a periodicity/ARNT/single-minded (PAS)-region serine residue. *Mol. Pharmacol.* **59,** 557–566.

Long, W. P., Chen, X., and Perdew, G. H. (1999). Protein kinase C modulates aryl hydrocarbon receptor nuclear translocator protein-mediated transactivation potential in a dimer context. *J. Biol. Chem.* **274,** 12391–12400.

Louis, M., and Becskei, A. (2002). Binary and graded responses in gene networks. *Sci. STKE* **2002,** PE33.

Martinez, J. M., Afshari, C. A., Bushel, P. R., Masuda, A., Takashi, T, and Walker, N. J. (2002). Differential toxicogenomic responses to 2,3,7,8-tetrachlorodibenzo-*p*-dioxin in malignant and nonmalignant human airway epithelial cells. *Toxicol. Sci.* **60,** 409–423.

Newlands, S., Levitt, L. K., Robinson, C. S., Karpf, A. B., Hodgson, V. R., Wade, R. P., and Hardeman, E. C. (1998). Transcription occurs in pulses in muscle fibers. *Genes Dev.* **12,** 2748–2758.

Park, S., Henry, E. C., and Gasiewicz, T. A. (2000). Regulation of DNA binding activity of the ligand-activated aryl hydrocarbon receptor by tyrosine phosphorylation. *Arch. Biochem. Biophys.* **381,** 302–312.

Rose'Meyer, R. B., Mellick, A. S., Garmham, B. G., Harrison, G. J., Massa, H. M., Griffiths, L. R. (2003). The measurement of adenosine and estrogen receptor expression in rat brains following ovariectomy using quantitative PCR analysis. *Brain Res. Protocols* **11,** 9–18.

Ross, I. L., Browne, C. M., and Hume, D. A. (1994). Transcription of individual genes in eukaryotic cells occurs randomly and infrequently. *Immunol. Cell. Biol.* **72,** 177–185.

Rossi, F. M., Kringstein, A. M., Spicher, A., Guicherit, O. M., and Blau, H. M. (2000). Transcriptional control: Rheostat converted to on/off switch. *Mol. Cell* **6,** 723–728.

Takasuka, N., White, M. R., Wood, C. D., Robertson, W. R., and Davis, J. R.

(1998). Dynamic changes in prolactin promoter activation in individual living lactotrophic cells. *Endocrinology* **139,** 1361–1368.

Tan, Z., Chang, X., Puga, A., and Xia, Y. (2002). Activation of mitogen-activated protein kinases (MAPKs) by aromatic hydrocarbons: Role in the regulation of aryl hydrocarbon receptor (AHR) function. *Biochem. Pharmacol.* **64,** 771–780.

Tritscher, A. M., Goldstein, J. A., Portier, C. J., McCoy, Z., Clark, G. C., and Lucier, G. W. (1992). Dose-response relationships for chronic exposure to 2,3,7,8-tetrachlorodibenzo-*p*-dioxin in a rat tumor promotion model: Quantification and immunolocalization of CYP1A1 and CYP1A2 in the liver. *Cancer Res.* **52,** 3436–3442.

Vanden Heuvel, J. P., Clark, G. C., Kohn, M. C., Tritscher, A. M., Greenlee, W. F., Lucier, G. W., Bell, D. A. (1994). Dioxin-responsive genes: Examination of dose-response relationships using quantitative reverse transcriptase-polymerase chain reaction. *Cancer Res.* **54,** 62–68.

White, M. R., Masuko, M., Amet, L., Elliott, G., Braddock, M., Kingsman, A. J., and Kingsman, S. M. (1995). Real-time analysis of the transcriptional regulation of HIV and hCMV promoters in single mammalian cells. *J. Cell Sci.* **108,** 441–455.

Whitlock, J. P. (1999). Induction of cytochrome P4501A1. *Annu. Rev. Pharmacol. Toxicol.* **39,** 103–125.

Wolfe, D. K. A., and Marquardt, H. (1995). Assessment of the cytotoxic and tumor promoting potential of 2,3,7,8-TCDD and PCB congeners *in vitro*: Comparison of *in vitro*- and *in vivo*-data. *Organohalogen Compounds* **25,** 195–198.